

Temperature-dependent 0.7 structure in the conductance of cleaved-edge-overgrowth one-dimensional wires

R. de Picciotto, L. N. Pfeiffer, K. W. Baldwin, and K. W. West
Bell Laboratories, Lucent Technologies, Murray Hill, New Jersey 07974, USA
 (Received 12 May 2005; published 22 July 2005)

We study the temperature dependence of the conductance in clean one-dimensional wires fabricated by cleaved-edge overgrowth in molecular beam epitaxy. At elevated temperatures, a conductance peculiarity occurs at low electron densities. The linear conductance dwells at a value of $\sim 70\%$ of its plateau value over a finite density range. We show that this so-called 0.7 structure arises as the electrons in the wire undergo a transition from a degenerate into a nondegenerate liquid.

DOI: [10.1103/PhysRevB.72.033319](https://doi.org/10.1103/PhysRevB.72.033319)

PACS number(s): 73.63.Nm, 73.23.Ad

One-dimensional (1D) ballistic wires possess unique electrical properties and have been the subject of numerous studies. Conduction in such wires is often discussed in the context of the Luttinger liquid model, which treats the interactions among electrons exactly and thus is expected to have a wide validity range. However, this model assumes that the energy available for elementary excitations remains within a narrow band about the Fermi energy E_F . It is thus applicable only at low temperatures, much lower than the Fermi temperature $T_F = E_F/k_B$, where k_B is Boltzmann's constant. Many of the properties of 1D wires at temperatures comparable to or even larger than T_F can be captured by the Landauer scattering approach. This method, however, ignores the interactions among electrons altogether. In this work we address the properties of 1D wires in this unusual parameter regime $T > T_F$.

The hallmark of ballistic electron transport in a 1D wire is the quantization of its linear conductance. In a multimode wire, the overall conductance is given by the conductance quantum $g_0 = 2e^2/h$, multiplied by the number of available 1D modes. Here e is the charge of an electron and h is Planck's constant. Such ballistic wires have been implemented in a multitude of material systems to date, including split-gate semiconductor quasi-1D quantum point contacts^{1,2} (QPCs) and wires,³ carbon nanotubes,⁴ and V-grooved⁵ or cleaved-edge-overgrowth AlGaAs heterostructures.⁶

With semiconductor-based wires, a voltage applied to a nearby gate readily controls the 1D charge density, and hence the number of occupied modes can be varied. Thus, the conductance of such ballistic wires exhibits a series of quantized conductance plateaus when plotted against the gate voltage. This quantization of the linear conductance in ballistic wires is a robust phenomenon—insensitive to the system details. All that is required is the absence of backward scattering inside the wire and adiabatic feeding of charge from the reservoirs into the wire.

At elevated temperatures the conductance may deviate from these integer values. Clearly, the temperature has to be lower than the intermode energy spacing Δ in order to resolve each mode. With semiconductor wires, the separation between the first and second modes can reach $T_\Delta = \Delta/k_B \sim 150$ K and thus temperatures lower than T_Δ can be routinely achieved, resulting in the aforementioned conductance plateaus.

In 1996, a surprising additional conductance step was noticed in the QPC data.⁷ At somewhat elevated temperatures and with low 1D densities, the conductance dwells at a value of $\sim 0.7g_0$ for a finite density range.⁷⁻¹⁷ This so-called 0.7 structure is a weak feature, distinct from the main plateau sequence. In QPC devices, it is observed at temperatures as low as a few kelvin, much smaller than T_Δ . Surprisingly, when the temperature is lowered further the effect becomes less pronounced and is absent in the lowest-temperature data ($T < 0.1$ K). The evolution of this structure with an applied source-drain bias, magnetic field, and temperature has led to a suggested link between this phenomenon, the spin degree of freedom,^{7,8} and the Kondo effect.^{16,18} Alternatively, an electron-phonon mechanism¹⁹ or Wigner crystallization²⁰ were also suggested as possible origins of this phenomenon.

Here we describe the temperature dependence of the conductance in a different 1D system. Using the cleaved-edge-overgrowth (CEO) technique,⁶ we fabricate long and ultra-clean ballistic quantum wires with a length-to-diameter ratio of ~ 100 , far larger than in QPC devices. We find that CEO wires share a 0.7-like structure with QPC devices. Our unique wires allow us to measure the specific capacitance of the device—which is found to be in excellent agreement with the one estimated from the known geometry. Thus, we can relate the applied gate voltage to the density in the wire and show that the 0.7 structure occurs whenever the temperature exceeds the Fermi temperature T_F .

Previous works^{21,22} have proven CEO wires to be ultra-clean, characterized by a long backscattering length that can exceed $20 \mu\text{m}$. The coupling of such CEO wires to their reservoirs, however, falls shy of ideal—leading to a somewhat larger contact resistance and a reduced two-terminal conductance per channel. Thus, the low-temperature conductance value at the first plateau ranges between 70% and 90% of the conductance quantum, depending on structure parameters (see Refs. 6, 21, and 22 for details). The wire itself, however, is ballistic and resistance-free, as verified by four-probe resistance measurements.²³

Conductance versus gate voltage traces, measured at various temperatures, are shown in Fig. 1. The 0.7 structure is clearly seen in the data. Similar to QPCs data, this feature becomes more pronounced at higher temperatures, with its density range increasing with temperature. A close inspection

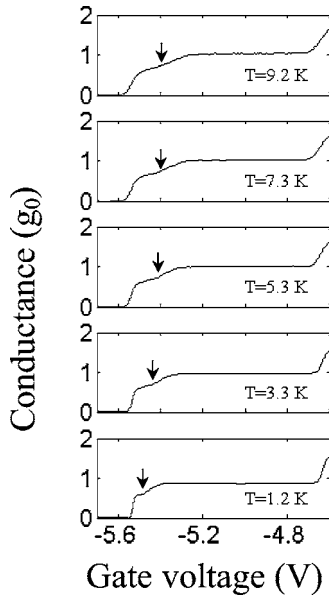


FIG. 1. Conductance vs gate voltage at different temperatures. The linear conductance of a 2- μm -long CEO wire, measured with an excitation of 30 μV at various temperatures, is plotted against the gate voltage. The conductance, divided here by the quantum conductance, dwells at a value of ~ 0.7 over a finite gate-voltage range. This conductance anomaly extends over a wider density range at higher temperatures (arrows).

of such traces shows that the value of the conductance at the first plateau, g_p , is by itself temperature dependent (not shown). It increases from $0.85g_0$ at $T \sim 0.3$ K and saturates to $g_p \approx g_0$ by $T \sim 10$ K for this wire.²⁴ This behavior, unique to CEO wires, results from the temperature dependence of the contact resistance.

In order to circumvent this temperature-dependent contact resistance, we plot in Fig. 2 the conductance, normalized to its plateau value, versus gate voltage at various temperatures. As can be seen in this figure, the conductance peculiarity always occurs at a conductance value of $\sim 0.66g_p$ regardless of temperature. Apparently, the value of the contact resistance itself is inconsequential.

To follow the evolution of this conductance feature with temperature, we measure the gate voltage V^* that marks the transition between the main plateau and the 0.7 structure (see Fig. 3). We thus define V^* as the gate voltage where the conductance equals 85% of its plateau value—halfway between 0.7 and 1—and follow its temperature dependence. As will be shown below, it is worthwhile to evaluate the Fermi energy at this gate voltage and discuss the temperature dependence of this Fermi energy. When the gate voltage equals V^* , the 1D density equals $n^* = (c/e)(V^* - V^{\text{th}})$, where V^{th} is the gate voltage required to deplete the wire at low temperatures ($T = 0.25$ K in this experiment) and c is the capacitance per unit length between the gate and the wire. This density, in turn, is related to the Fermi wave vector via $k_F^* = \frac{1}{2}\pi n^*$, with the factor $\frac{1}{2}$ accounting for spin degeneracy. Thus, once the specific capacitance is known, the Fermi energy at this gate voltage can be readily calculated as $E_F^* = \hbar^2(k_F^*)^2/2m$, where m is the band mass.

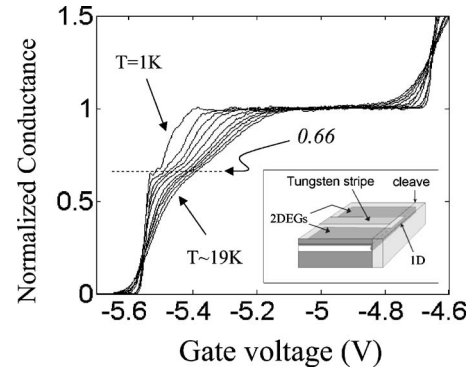


FIG. 2. Normalized conductance vs gate voltage at different temperatures. The conductance, normalized to its value at the first plateau g_p , is plotted against the gate voltage. The temperature ranges from 1 to 19 K with 2 K increments between traces. The anomaly occurs at a conductance of 66–68 % of the plateau value, regardless of temperature. Inset: Geometry of a CEO wire. A two-dimensional electron gas (2DEG) is formed in a 25 nm GaAs quantum well by modulation doping. The resultant 2DEG has a carrier density $n_s \approx 2.5 \times 10^{11} \text{ cm}^{-2}$, and mobility $\mu \approx 4 \times 10^6 \text{ cm}^2/\text{Vs}$. A second modulation doping sequence is then grown onto a freshly cleaved [011] facet to create the 1D wire along the cleaved edge. A tungsten gate evaporated onto the top surface is utilized to deplete the 2DEG and separate out the wire in front of it. The resultant two separate 2DEG sheets are used as source and drain reservoirs.

To determine this capacitance, we performed nonlinear transport measurements in the same wire, as shown in the inset of Fig. 3. In a recent work,¹⁷ we used such data, in conjunction with a simple model, to determine this specific capacitance and show that the 0.7 structure occurs in the low-temperature differential conductance when a bias as large as four times the Fermi energy is applied across the wire. Here we use the same method to measure this capacitance, which is then used to establish the Fermi energy.

In Fig. 4 we plot E_F^* , deduced from the measured gate voltage V^* , against temperature for the two different wires measured. As can be seen in this figure, this quantity is simply proportional to temperature. Moreover, the coefficient of proportionality equals unity, namely, $E_F^* = k_B T$, as illustrated by the solid line in the same figure. Thus, the crossover from the conductance plateau into the 0.7 structure occurs as the 1D carriers are diluted to form a nondegenerate system.

To further analyze the data, we measure another characteristic gate voltage V' , which corresponds to the extent of the 0.7 structure itself (see Fig. 3). Since the 0.7 structure in our wires occurs when the conductance equals 66–68% of the plateau value, we defined V' as the gate voltage where the normalized conductance equals 0.69. In other words, V' is defined such that the conductance anomaly occurs in the density range $0 \leq n \leq n(V_{\text{gate}} = V')$.²⁶ We plot the corresponding Fermi energy against temperature in the same figure. Clearly, the 0.7 structure occurs deep in the nondegenerate regime. We find that the density band matching $0 \leq E_F(n) \leq 0.4k_B T$ describes the range where the 0.7 structure occurs fairly accurately, as can be seen in Fig. 4.

With free electrons in a reflection-free single-mode wire, the well-known cancellation between the velocity and the

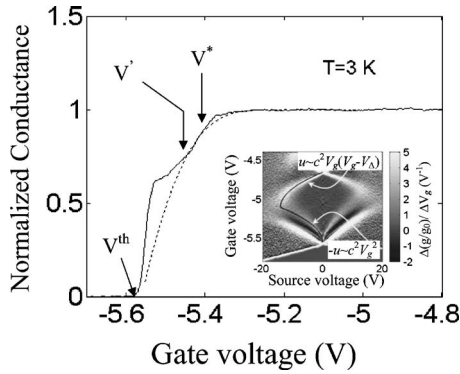


FIG. 3. Characteristics of the 0.7 structure. The conductance at $T=3$ K, normalized to its plateau value, is plotted against the gate voltage. Two characteristic gate voltages are indicated: V^* corresponds to the transition between the plateau and the 0.7 structure, and V' marks the high-density extent of this feature (see text). The threshold gate voltage V^{th} is also indicated. Dotted line: the expected conductance within a free-electron model (see text). Inset: Transconductance vs gate voltage and dc bias. The numerical derivative of the differential conductance with respect to gate voltage as a function of gate voltage and dc bias, in a gray-scale format. Data were taken with an ac excitation of $30 \mu\text{V}$ at a bath temperature of 250 mK. The light lines separate regions of different conductance values. The central dark region, where this derivative vanishes, corresponds to the first plateau. Superimposed on the data are two curves (black lines): the upper curve $u_{\Delta}=4(E_F/e)(1-\sqrt{\Delta/E_F})$ marks the onset of the second subband transport at high densities, and the lower curve $u_0=-4E_F/e$ marks the boundary between the plateau and the 0.7 structure. These fitted curves, bounding the plateau region, are used to deduce the specific capacitance (see Ref. 17 for details). The deduced values were $c=18.0\pm 0.5$ pF/m for the data shown and 19.0 ± 0.5 pF/m for the second wire measured (data included in Fig. 4).

density of states leads to a simple expression for the linear conductance:

$$g/g_0 = \int_0^{\infty} d\varepsilon \frac{f(\varepsilon - eu/2) - f(\varepsilon + eu/2)}{eu} \\ \times \xrightarrow{u \rightarrow 0} \int_0^{\infty} d\varepsilon \left(-\frac{\partial f}{\partial \varepsilon} \right) = f(0).$$

Here u is the applied source-drain bias and $f(\varepsilon)$ is the Fermi function. Thus, in this simple model, the conductance equals the value of the Fermi function when evaluated at zero energy: $f(0)=1/(1+e^{-\mu/k_B T})$.²⁷ The chemical potential μ is related to both temperature and the applied gate voltage via

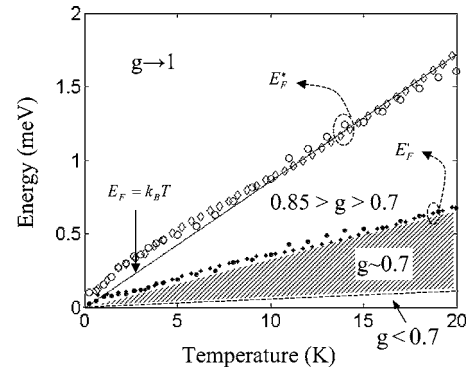


FIG. 4. Phase diagram of the 0.7 structure. The Fermi energy in the wire at the transition between the plateau and the 0.7 structure, $E_F^*=E_F(V_{\text{gate}}=V^*)$ (open symbols) and the one marking the high-density edge of this feature, $E_F'=E_F(V_{\text{gate}}=V')$ (filled symbols) are plotted against temperature. Data were taken from two different wires, both $2 \mu\text{m}$ long (diamonds and circles). The measured gate voltages were translated into Fermi energies, using the expression for spin-degenerate free electrons in 1D (Ref. 25). The data appear linear in this energy-temperature plane, attesting to the 1D nature of our device. The line $E_F=k_B T$ is added onto the data (solid line). The shaded area at the bottom of the figure corresponds to the 0.7 structure region—clearly in the nondegenerate regime. The measured conductance dwells at $g \sim 0.7$ down to very low 1D densities (Ref. 26), as illustrated by the dashed line.

$n = \int_0^{\infty} d\varepsilon [\nu(\varepsilon) f((\varepsilon - \mu)/k_B T)] = (c/e)(V_{\text{gate}} - V_{\text{th}})$ where $\nu(\varepsilon) = 2/h\sqrt{2m/\varepsilon}$ is the density of states.

We have evaluated this chemical potential and added the resultant conductance trace onto the data in Fig. 3. Evidently, the fact that the conductance decreases significantly below its plateau value as the gate voltage is reduced to V^* , where $E_F=k_B T$, is not very surprising and is in fact expected from this model. The surprising feature is the *excess of conductance* at lower densities. Similar to the nonlinear response at low temperatures,¹⁷ here again the measured conductance is *too high* to be accounted for by a free-electron model.²⁵

To summarize, we have measured the temperature dependence of the conductance in clean and long CEO wires and found a 0.7-like structure. We show that this phenomenon occurs when the temperature exceeds the Fermi energy by a factor of $\sim 2^{1/2}$. We also show that the 0.7 structure amounts to an excess of measured conductance, not accounted for in a model that ignores the electron-electron interactions.

R.d.P. thanks A. M. Finkel'stein, A. Punnoose, S. H. Simon, C. M. Varma, and N. Zhitenev for stimulating discussions.

¹B. J. van Wees, H. van Houten, C. W. J. Beenakker, J. G. Williamson, L. P. Kouwenhoven, and D. van der Marel, Phys. Rev. Lett. **60**, 848 (1988).

²D. A. Wharam, T. J. Thornton, R. Newbury, M. Pepper, H. Ahmed, J. E. F. Frost, D. G. Hasko, D. C. Peacock, D. A.

Ritchie, and G. A. C. Jones, J. Phys. C **21**, L209 (1988).

³S. Tarucha, T. Honda, and T. Saku, Solid State Commun. **94**, 413 (1995).

⁴S. J. Tans, A. R. M. Verschueren, and C. Dekker, Nature (London) **393**, 49 (1998).

- ⁵D. Kaufman, Y. Berk, B. Dwir, A. Rudra, A. Palevski, and E. Kapon, Phys. Rev. B **59**, R10433 (1999).
- ⁶L. N. Pfeiffer, A. Yacoby, H. L. Stormer, K. W. Baldwin, J. Hasen, A. Pinczuk, W. Wegscheider, and K. W. West, Microelectron. J. **28**, 817 (1997).
- ⁷K. J. Thomas, J. T. Nicholls, M. Y. Simmons, M. Pepper, D. R. Mace, and D. A. Ritchie, Phys. Rev. Lett. **77**, 135 (1996).
- ⁸N. K. Patel, J. T. Nicholls, L. Martin-Moreno, M. Peper, J. E. F. Forst, D. A. Ritchie, and G. A. C. Jones, Phys. Rev. B **44**, 10973 (1991).
- ⁹B. E. Kane, G. R. Facer, A. S. Dzurak, N. E. Lumpkin, R. G. Clark, L. N. Pfeiffer, and K. W. West, Appl. Phys. Lett. **72**, 3506 (1998).
- ¹⁰K. J. Thomas, J. T. Nicholls, N. J. Appleyard, M. Y. Simmons, M. Pepper, D. R. Mace, W. R. Tribe, and D. A. Ritchie, Phys. Rev. B **58**, 4846 (1998).
- ¹¹A. Kristensen, P. E. Lindelof, J. B. Jensen, M. Za'alon, J. Hollingbery, S. W. Pedersen, J. Nygard, H. Bruus, S. M. Reimann, C. B. Sørensen, M. Michel, and A. Forchel, Physica B **249–251**, 180 (1998).
- ¹²K. S. Pyshkin, C. J. B. Ford, R. H. Harrell, M. Pepper, E. H. Linfield, and D. A. Ritchie, Phys. Rev. B **62**, 15842 (2000).
- ¹³S. Nuttinck *et al.*, Jpn. J. Appl. Phys., Part 2 **39**, L655 (2000).
- ¹⁴A. Kristensen, H. Bruus, A. E. Hansen, J. B. Jensen, P. E. Lindelof, C. J. Marckmann, J. Nygard, C. B. Sørensen, F. Beuscher, A. Forchel, and M. Michel, Phys. Rev. B **62**, 10950 (2000).
- ¹⁵D. J. Reilly, G. R. Facer, A. S. Dzurak, B. E. Kane, R. G. Clark, P. J. Stiles, R. G. Clark, A. R. Hamilton, J. L. O'Brien, N. E. Lumpkin, L. N. Pfeiffer, and K. W. West, Phys. Rev. B **63**, 121311 (2001).
- ¹⁶S. M. Cronenwett, H. J. Lynch, D. Goldhaber-Gordon, L. P. Kouwenhoven, C. M. Marcus, K. Hirose, N. S. Wingreen, and V. Umansky, Phys. Rev. Lett. **88**, 226805 (2002).
- ¹⁷R. de Picciotto, L. N. Pfeiffer, K. W. Baldwin, and K. W. West, Phys. Rev. Lett. **92**, 036805 (2004).
- ¹⁸Y. Meir, K. Hirose, and N. S. Wingreen, Phys. Rev. Lett. **89**, 196802 (2002).
- ¹⁹Georg Seelig and K. A. Matveev, cond-mat/0211579 (unpublished).
- ²⁰K. A. Matveev, Phys. Rev. Lett. **92**, 106801 (2004).
- ²¹A. Yacoby, H. L. Stormer, Ned S. Wingreen, L. N. Pfeiffer, K. W. Baldwin, and K. W. West, Phys. Rev. Lett. **77**, 4612 (1996).
- ²²R. de Picciotto, H. L. Stormer, A. Yacoby, K. W. Baldwin, L. N. Pfeiffer, and K. W. West, Phys. Rev. Lett. **85**, 1730 (2000).
- ²³R. de Picciotto, H. L. Stormer, L. N. Pfeiffer, K. W. Baldwin, and K. W. West, Nature (London) **411**, 51 (2001).
- ²⁴The conductance saturates to a value that exceeds g_0 by 4% for the wire shown in Fig. 1. This also occurred to a greater extent ($\sim 7\%$) with the second wire studied here. This peculiar behavior will be the subject of a separate study.
- ²⁵This is true irrespective of spin polarization, as the existence of a spin gap will further reduce the expected value of the conductance. It is possible to obtain agreement between a spin-gap model and the data *over a limited density range*, by using the capacitance as a fitting parameter. However, the capacitance deduced in this way, about twice the measured one, leads to an unreasonably large value for the gap between the first and second subbands, $\Delta \sim 600$ K, as opposed to $\Delta \sim 160$ K evaluated by using the independently measured capacitance. Such a gap between the subbands is inconsistent with known device parameters. Therefore spin polarization cannot account for our data.
- ²⁶The conductance declines toward zero when the density in the wire is very small, 2–3 times smaller than the one at the high-density edge of the 0.7 structure. Therefore, this feature extends to a Fermi energy as small as $\sim k_B T/15$.
- ²⁷A. Punnoose and S. H. Simon are thanked for pointing out this simple fact.